Coupled Dynamics of Photosynthesis, Transpiration, and Soil Water Balance. Part II: Stochastic Analysis and Ecohydrological Significance

EDOARDO DALY

Dipartimento di Idraulica Trasporti e Infrastrutture Civili, Politecnico di Torino, Turin, Italy, and Department of Civil and Environmental Engineering and Princeton Environmental Institute, Princeton University, Princeton, New Jersey

AMILCARE PORPORATO

Department of Civil and Environmental Engineering, Duke University, Durham, North Carolina

IGNACIO RODRIGUEZ-ITURBE

Department of Civil and Environmental Engineering and Princeton Environmental Institute, Princeton University, Princeton, New Jersey

(Manuscript received 20 May 2003, in final form 16 December 2003)

ABSTRACT

The coupled dynamics of soil moisture, transpiration, and assimilation are studied at the daily time scale by temporally upscaling the hourly time scale results obtained in a companion paper. The effects of soil and vegetation characteristics on soil moisture dynamics at the daily time scale and the parameters characterizing the dependence of transpiration and assimilation on soil water content are analyzed and discussed. The daily leaf carbon assimilation is then coupled to a stochastic soil moisture model to obtain a probabilistic description of the carbon assimilation during a growing season. The rainfall regime, in terms of both frequency and amount of precipitation, controls the mean assimilation during a growing season that reaches a maximum for an intermediate range of daily rainfall probabilities, indicating the existence of a rainfall regime that is most effective for plant productivity. The analysis of the duration and frequency of periods of no assimilation provides a measure of plant water stress as a function of the soil, vegetation, and climate characteristics. The results are in good agreement with the dynamic water stress defined in Porporato et al. on the basis of the crossing properties of the stochastic soil moisture dynamics.

1. Introduction

When temperature and nutrient availability are not controlling factors, the soil moisture is the key environmental variable at the basis of vegetation dynamics. The temporal evolution of soil water availability directly controls the plant water potential, the related tissue turgor, the transpiration rate, and the leaf carbon assimilation by photosynthesis, which, in turn, impacts the plant growth and reproduction (e.g., Rodriguez-Iturbe et al. 2001; Porporato et al. 2001; Porporato and Rodriguez-Iturbe 2002). The dynamics of plant water potential as well as that of transpiration and assimilation rates have marked diurnal fluctuations that are modulated by soil moisture dynamics whose crucial features evolve on a longer (i.e., daily) time scale. The short-term variability resulting from the diurnal solar forcing affects plant conditions primarily through its daily averaged impact on the soil water balance. To pinpoint the essential interactions between hydrological processes and vegetation it is thus convenient to bypass the diurnal fluctuations and focus on the behavior of their mean daily values.

In this paper, starting from the integration of the results of a suitable model at the hourly time scale (Daly et al. 2004, hereafter Part I), the functional dependence of daily transpiration and net carbon assimilation on relative soil moisture is found to follow regular behaviors that allow simple parameterizations in terms of the climate, soil, and vegetation characteristics of the original hourly time scale model. In particular, the similarity of the obtained transpiration function with the empirical one often used in the daily time scale models of soil moisture dynamics (e.g., Cordoba and Bras 1981; Dingman 1994; Rodriguez-Iturbe et al. 1999; Laio et al. 2001b) and the analogous link between plant carbon assimilation and soil moisture offer a new interpretation of such models and reinforce their previous results. The functional dependence of daily transpiration and assimilation on soil moisture is then embedded into a sto-

Corresponding author address: Dr. Amilcare Porporato, Dept. of Civil and Environmental Engineering, 127 Hudson Hall, Duke University, Durham, NC 27708.
E-mail: amilcare@duke.edu

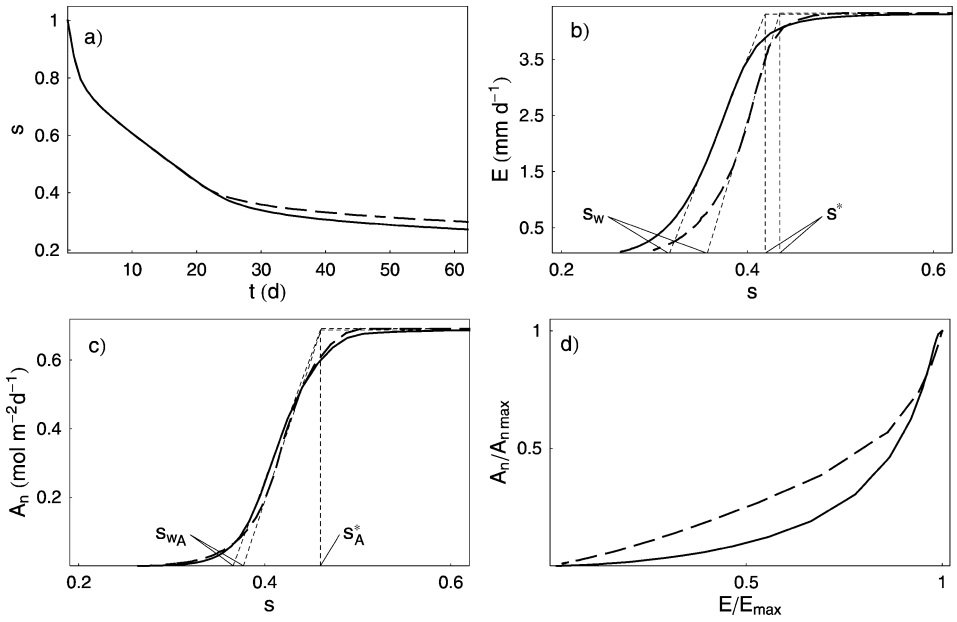

FIG. 1. Results at daily time scale for Jarvis's approach (continuous line) and Leuning's formulation (dashed line): (a) relative soil moisture during a drying period; (b), (c) respectively, daily transpiration and daily net assimilation as a function of relative soil moisture (the approximating piecewise functions are shown with dotted line; see text for details); and (d) relation between assimilation and transpiration. Loamy soil, $R_{AI} = 5.6$, $L_{AI} = 1.4$, and soil depth $Z_r = 60$ cm. For vegetation and soil parameters, refer to Tables 1, 2, and 3 in Part I.

chastic soil moisture model (e.g., Rodriguez-Iturbe et al. 1999; Laio et al. 2001b) to analyze the impact of rainfall intermittency on the dynamics of plant carbon assimilation.

2. Daily time scale dynamics

As discussed in Part I, the diurnal patterns of transpiration and assimilation are strongly controlled by the values of soil water potential. The mean daily values of transpiration and assimilation are thus expected to be characterized by regular and relatively simple relationships with soil moisture dynamics.

Examples of the integrated processes obtained from the results at the hourly time scale (section 5 of Part I) are shown in Figs. 1 and 2. The vegetation parameters used in the simulations are typical of a C_3 woody plant adapted to a semiarid climate (e.g., Scholes and Walker 1993). The mean daily values of soil moisture during the drying phase are observed to follow a very similar pattern to those at the hourly time scale. More interesting, the behavior of transpiration, shown in Figs. 1b and 2a, is found to closely resemble the empirical relationship often employed in hydrologic and ecologic models at the daily time scale (e.g., Cordoba and Bras 1981; Dingman 1994; Paruelo and Sala 1995; Rodriguez-Iturbe et al. 1999; Laio et al. 2001b), where transpiration is approximated as a piecewise function of relative soil moisture, s, constant above a certain s^* and linearly decreasing to zero at the so-called wilting point, s_w; that is,

$$E(s) = \begin{cases} 0 & s \le s_w \\ \dfrac{s - s_w}{s^* - s_w} E_{\max} & s_w \le s \le s^* \\ E_{\max} & s^* < s \le 1, \end{cases} \qquad (1)$$

where $E_{\max}$ is the daily transpiration rate under well-watered conditions. Thanks to its derivation from the hourly time scale model, which is more specific from a physical point of view, this result offers a sounder justification of the previously mentioned models of soil moisture dynamics and is similar to the results reported by Federer (1979). Moreover, as discussed in detail in the next section, the three parameters of the daily transpiration function (i.e., s_w, s^*, and $E_{\max}$) become connected by the temporal upscaling to the plant, soil, and climate characteristics.

A behavior similar to that of daily transpiration is also found for the dependence of daily carbon assimilation on soil moisture (Figs. 1c and 2b), which may be approximated as

$$A_n(s) = \begin{cases} 0 & s \le s_{w_A} \\ \dfrac{s - s_{w_A}}{s^*_A - s_{w_A}} A_{\max} & s_{w_A} \le s \le s^*_A \\ A_{\max} & s^*_A < s \le 1. \end{cases} \qquad (2)$$

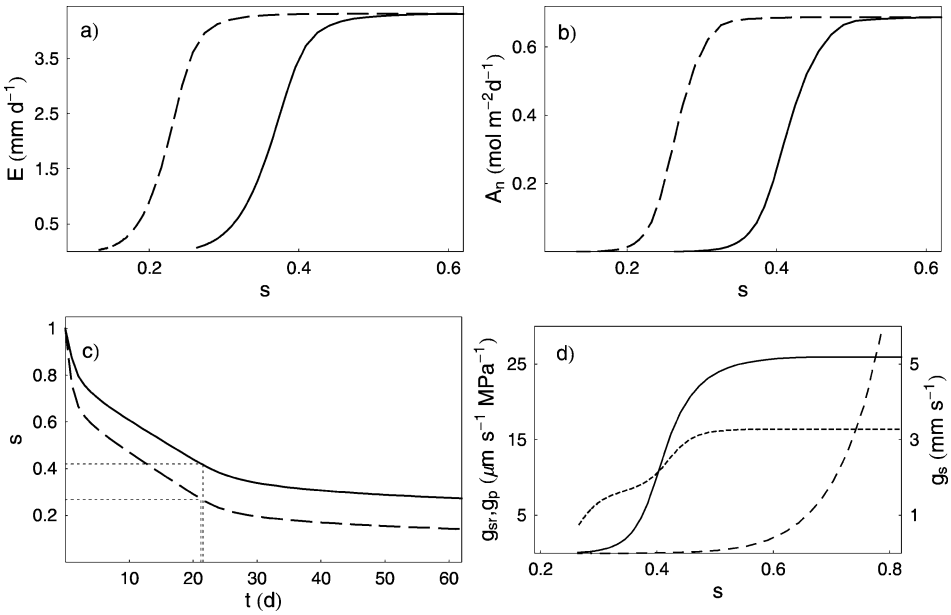

FIG. 2. Influence of soil type on (a) mean daily transpiration, (b) mean daily assimilation, and (c) mean daily soil moisture using Jarvis's approach: loam (continuous line) and loamy sand (dashed line). Dotted lines in (c) show the times after which soil moisture reaches s^* with the two considered soil types. (d) Comparison of different mean daily conductances for a loam with $Z_r = 60$ cm: stomatal conductance (continuous line), soil–root conductance (dashed line), and plant conductance (dotted line). See caption of Fig. 1 for other parameters.

Such a relationship is key to link photosynthesis and assimilation to the probabilistic description of soil moisture dynamics at the daily time scale (see sections 4 and 5). Owing to the direct effects of low leaf water potential on the chemical reactions of photosynthesis, the values of s_{w_A} and s_A^* in Eq. (2) are slightly higher than the corresponding points for transpiration. The relation between E and A_n (Fig. 1d) shows a nonlinear behavior linked to the faster decrease of A_n compared to that of E at low soil moisture. This difference is less marked with Leuning's (1990, 1995) formulation because, in that case, E is related to A_n through g_s.

Jarvis's (1976) and Leuning's approaches give almost the same values of s_{w_A} and s_A^*, while for Leuning's formulation the assimilation rate under stressed conditions is lower (Fig. 1c), and s_w and s^* are higher. This is probably an artifact in Leuning's formulation that could be solved by making the parameter a_1 of Eq. (14) in Part I a function of soil moisture. In what follows we only consider Jarvis's formulation for its simplicity. In any case, the qualitative similarity of the results of the two approaches gives confidence about the robustness of the hourly time scale model, whose integrated response at the daily time scale proves to be independent of the details at the hourly time scale and in particular of the specific (e.g., Jarvis's or Leuning's) formulation of the stomatal function. It is important to remark that a direct estimation from field data of the parameters of the daily time scale model is required for the quantitative analysis of specific ecosystems to account for complex spatial and temporal variability of the soil–plant–atmosphere dynamics (Wetzel and Chang 1987, 1988; Crow and Wood 2002).

3. Physical interpretation of the parameters

Before proceeding with the analysis of the links between photosynthesis and soil moisture dynamics at the daily level, it is interesting to analyze in detail the dependence of the parameters of the transpiration and assimilation functions on soil and vegetation characteristics. Figures 2a and 2b show the impact of two different soil types on soil moisture dynamics. As expected, soil properties, especially hydraulic conductivity and soil texture, control transpiration through their influence on both soil–root conductance and soil water potential. Plants in soils with higher K_s tend to have lower s^*, because of the lower soil resistance to water uptake and transpiration, but reach s^* approximately at the same time because of the faster soil moisture depletion (Fig. 2c), due to the higher leakage. The soil type has negligible influence on the maximum transpiration and assimilation rates, which essentially only depend on the leaf–plant conductances that are dominating under well-watered conditions.

The plant type may have an important effect on the value of s^* through the root and leaf area index, the maximum leaf–plant conductances, and the thresholds controlling stomatal functioning and photosynthesis. Although the role of R_{AI} and L_{AI} is modeled very simply

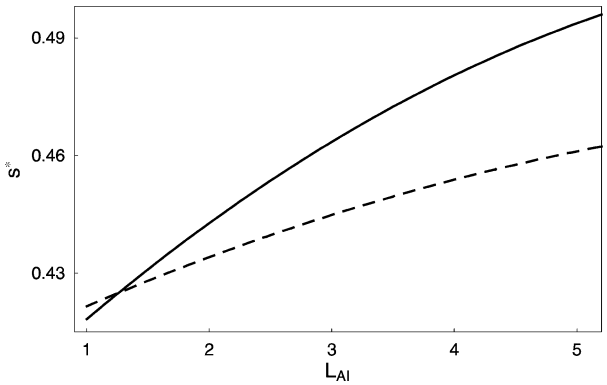

FIG. 3. Influence of root area index and leaf area index on s^*. Continuous line represents constant $R_{AI} = 5.6$, while the dashed line is for constant $R_{AI}/L_{AI} = 4$. Soil type is a loam with $Z_r = 60$ cm; plant parameters are typical of a C_3 plant adapted to semiarid conditions (see Tables 1, 2, and 3 in Part I).

in Part I, some general comments are possible. As shown in Fig. 3, the root area index (R_{AI}) has some impact on the resulting value of s^*, because a decrease in R_{AI} reduces the soil–root conductance and thus s^* increases, while the leaf area index (L_{AI}) has a greater influence on s^* for its direct control on transpiration. A higher L_{AI} causes a faster soil drying accompanied by higher values of s^* (Fig. 3) so that, when plants allocate more biomass to leaves than to roots, their sensibility to water deficit is increased. On the other hand, since an increase in L_{AI} implies higher transpiration rates and an earlier onset of water stress, a plant maintaining a constant R_{AI}/L_{AI} has lower s^* variability even with a high leaf area index and, therefore, is probably less sensitive to water stress. The strategy of allocating more biomass in the leaves in humid conditions to achieve higher assimilation rates and of preferentially allocating biomass in the roots in arid environments for a better soil water use (Larcher 1995, p. 143) supports these observations. The value of s^* is also conditioned by ψ_{l_1}, that is, the leaf water potential level at which stomata start closing in Jarvis's formulation (see Part I for details). Low values of ψ_{l_1}, which are typical of plants with high resistance to water stress, correspond to low values of s^* when all the other parameters are the same.

If s^* appears to be significantly affected by R_{AI} and L_{AI}, these two indexes do not seem to influence s_w very much, which instead mainly depends on K_s through g_{sr}, which is the first conductance to become limiting at low soil moisture levels (Fig. 2d). The plant influence on s_w occurs through ψ_{l_0}, the leaf water potential corresponding to complete stomata closure (i.e., $g_s = 0$) and to widespread xylem cavitation (i.e., $g_p \sim 0$). In a similar way, s_{w_A} is strongly influenced by the combined effect of ψ_{l_1} and $\psi_{l_{A_1}}$, that is, the values at which the leaf water potential starts affecting, respectively, stomata movement and net assimilation (see Part I for details). A reduction in $\psi_{l_{A_1}}$ lowers the water potential at which the chemical reactions of photosynthesis start being impaired. This in turn increases the steepness of the curve A_n versus s in the tract between s_{w_A} and s_A^*.

Finally, analysis not reported here shows that the maximum transpiration and assimilation rates, E_{max} and A_{max}, essentially depend on both vegetation type, through the physiological parameters g_{smax} and g_{pmax}, and the atmospheric boundary layer conditions.

4. Probabilistic dynamics of carbon assimilation during a growing season

The previous description of the daily dynamics of soil moisture, transpiration, and carbon assimilation during interstorm periods is now extended to include stochastic rainfall fluctuations. As in Rodriguez-Iturbe et al. (1999) and Laio et al. (2001b), the description of the rainfall model and the resulting infiltration takes advantage of the physical interpretation at the daily time scale at which the internal storm structure is not important and the soil moisture conditions are assumed to instantaneously adapt to the intermittent rainfall input. Thus, at the daily time scale, the previous soil moisture model remains valid during randomly varying interstorm periods, provided the initial conditions are properly updated according to the stochastic infiltration dynamics.

Following Rodriguez-Iturbe et al. (1999), the rainfall input is modeled as a marked Poisson process whose events take place with rate λ and carry a random depth of water with exponential distribution of mean α. Canopy interception is modeled by reducing the effective rainfall frequency as $\lambda' = \lambda e^{-\Delta/\alpha}$, where Δ is the maximum rainfall depth intercepted by each event (Rodriguez-Iturbe et al. 1999) and depends on L_{AI} and plant type. The increment in soil moisture due to infiltration from a rainfall event is assumed to be equal to the rainfall depth of that particular event when it does not exceed the available soil storage, otherwise the excess is considered to be converted in surface runoff.

Under the previous assumptions, the equation for the vertically averaged soil moisture dynamics at the daily time scale is

$$nZ_r \frac{ds(t)}{dt} = I[s(t), t] - E[s(t)] - \mathrm{EV}[s(t)] - L[s(t)], \qquad (3)$$

where n is porosity, Z_r is root depth, $I[s(t), t]$ is the infiltration rate after subtraction of runoff and interception losses, and transpiration $E[s(t)]$ is a function of s according to Eq. (1). Soil evaporation is as in Part I, and leakage is modeled as in Laio et al. (2001b) using an exponential function to simplify analytical developments.

For rainfall and evapotranspiration parameters representative of a typical growing season, the steady-state probability density function (pdf) of soil moisture can be obtained analytically as (Rodriguez-Iturbe et al. 1999)

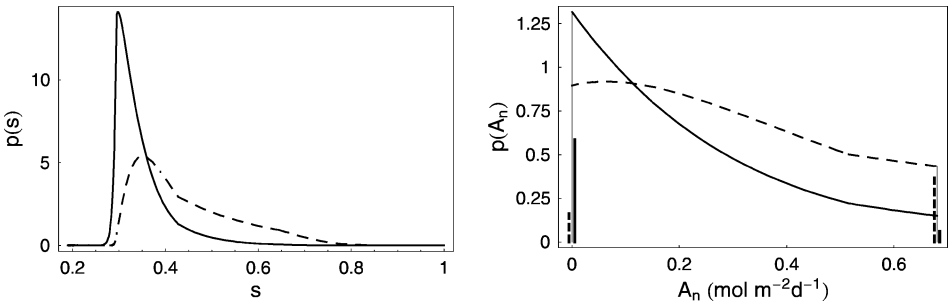

FIG. 4. Probability density function of soil moisture and assimilation as a function of frequency of rainfall events ($\lambda = 0.15$, continuous line; $\lambda = 0.3$, dashed line). The vertical bars are the atoms of probability in zero and $A_{\max}$. Soil type is a loam with $Z_r = 60$ cm; $E_{\max} = 4.3$ mm day^{-1}, $L_{\text{AI}} = 1.4$, $R_{\text{AI}} = 5.6$, $A_{\max} = 0.68$ mol m^{-2} day^{-1}, $s_w = 0.29$, $s^* = 0.43$, $s_{w_A} = 0.34$, and $s_A^* = 0.45$.

$$p(s) = \frac{C}{\rho(s)} \exp\left[-\gamma s + \lambda' \int_s \frac{du}{\rho(u)}\right], \qquad (4)$$

where C is a normalization constant and $\rho(s)$ is the normalized sum of the losses, that is, $\rho(s) = \{E[s(t)] + \text{EV}[s(t)] + L[s(t)]\}/nZ_r$.

Since the pdfs of s and $E(s)$ have been investigated in detail by Laio et al. (2001b), here we concentrate on the probabilistic structure of the daily assimilation, A_n. The pdf of A_n, easily obtained as a derived distribution of $p(s)$, has an atom of probability in zero, $P_{A_0} = \int_0^{s_{w_A}} p(s)\, ds$; one in $A_{\max}$, $P_{A_{\max}} = \int_{s_A^*}^1 p(s)\, ds$; and is continuous in between. The two atoms of probability represent, respectively, the fraction of time during a growing season in which soil moisture is too low for a plant to perform photosynthesis and the fraction of time when the plant achieves maximum assimilation. The probability $P_{A_{\text{st}}} = \int_{s_{w_A}}^{s_A^*} p(s)\, ds$ is the average fraction of time in a growing season in which assimilation takes place in nonoptimum (i.e., stressed) conditions. These statistics, through the soil moisture dynamics, synthesize the action of climate, soil, and vegetation characteristics on plant photosynthesis and carbon assimilation. Figure 4 shows an example of pdfs of s and A_n for two different climatic conditions. In arid climates, the low soil moisture values cause a higher P_{A_0} value and a fast decrease of $p(A_n)$ for high A_n values, while in wetter climates $P_{A_{\max}}$ is higher and the decrease of $p(A_n)$ with A_n is slower.

The impact of the rainfall regime, both in terms of total amounts per growing season and as a function of the frequency and amount of rainfall per event, may be studied by varying the parameters λ and α. Figure 5a shows the effect of increasing the total rainfall by varying λ while keeping α constant. As expected, a greater water availability increases the probability of maximum assimilation rate, $P_{A_{\max}}$ and lowers the total time of zero assimilation, P_{A_0}. Interestingly, the maximum of assimilation under stressed conditions, $P_{A_{\text{st}}}$, roughly corresponds to a rainfall regime for which previous analysis based on the crossing analysis of soil moisture (e.g., Porporato et al. 2001, 2003) found the transition between stressed and unstressed plant conditions.

Figure 5b shows the result of the probability of assimilation when the total rainfall is kept constant but the frequency and the mean depth of rainfall events are changed. A maximum in the probability of both stressed and unstressed assimilation is present. In particular, a maximum in $P_{A_{\max}}$ for the same total rainfall implies a maximum in the efficiency of the rainfall regime for assimilation and photosynthesis. Further analysis of the water balance (not reported here) shows that in such conditions runoff and interception losses are low com-

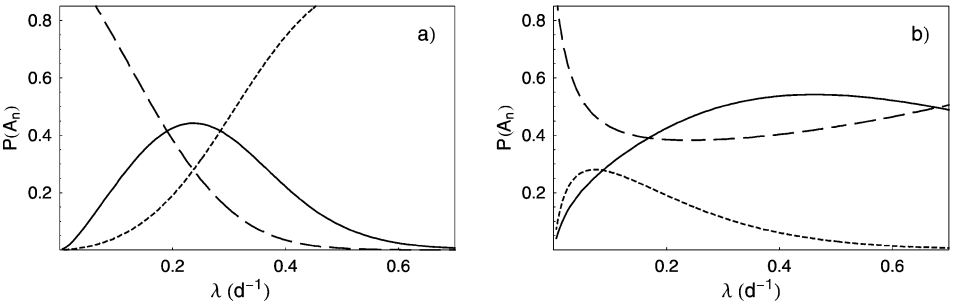

FIG. 5. Probabilities of assimilation rate, P_0 (dashed line), $P_{A_{\text{st}}}$ (continuous line), and $P_{A_{\max}}$ (dotted line) as a function of frequency of rainfall λ (a) for a given rainfall depth ($\alpha = 1.5$ cm) and (b) for constant mean total rainfall ($\Theta = 60$ cm) during a growing season ($T_{\text{seas}} = 200$ days, $\Delta = 0.2$ cm). Soil type is a loam with $Z_r = 60$ cm; $E_{\max} = 4.3$ mm day^{-1}, $L_{\text{AI}} = 1.4$, $R_{\text{AI}} = 5.6$, $A_{\max} = 0.68$ mol m^{-2} day^{-1}, $s_w = 0.29$, $s^* = 0.43$, $s_{w_A} = 0.34$, and $s_A^* = 0.45$.

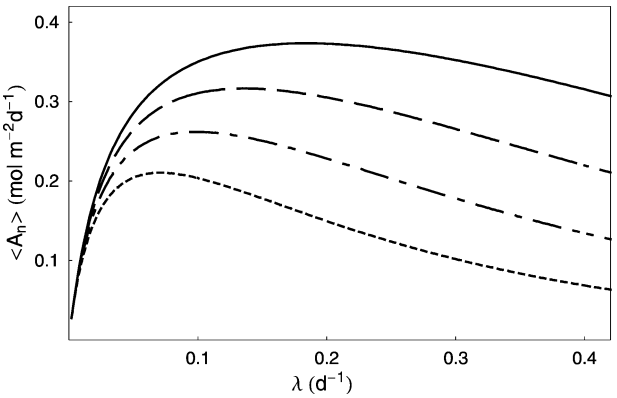

FIG. 6. Mean assimilation rate as a function of frequency of rainfall events for different total rainfall in a growing season (Θ = 80-cm continuous line, 70-cm dashed line, 60-cm chain line, and 50-cm dotted line). Soil type is a loam with Z_r = 60 cm; $E_{\max}$ = 4.3 mm day^{-1}, L_{AI} = 1.4, R_{AI} = 5.6, $A_{\max}$ = 0.68 mol m^{-2} day^{-1}, s_w = 0.29, s^* = 0.43, s_{w_A} = 0.34, and s_A^* = 0.45.

pared to transpiration and, at the same time, the soil moisture is at a level that allows the plant to maintain relatively high water potential and hence sufficient levels of tissue turgor, hydration, and photosynthesis.

5. Mean carbon assimilation and plant water stress

Although A_n does not take into account the carbon lost by plant respiration (see Part I), the net carbon assimilation at the leaf level can be considered an index of plant productivity. In this respect, the analysis of the mean assimilation during a growing season, $\langle A_n \rangle = \int_0^{A_{\max}} A_n p(A_n)\, dA_n$, assumes a particular interest.

Figure 6 shows the interplay between the timing and the amount of rainfall and $\langle A_n \rangle$. Similarly to the results in Fig. 5b, net assimilation reaches a maximum at intermediate values of λ. Increasing the mean total rainfall Θ induces higher $\langle A_n \rangle$, but also shifts the maximum toward higher values of λ. For a given type of soil and vegetation, a maximum in $\langle A_n \rangle$ is linked to the efficiency of the rainfall regime and recalls the results of Laio et al. (2001b) and Porporato et al. (2001), who reported the existence of optimal plant conditions, in terms of transpiration and water stress, for average conditions of frequency and amounts of rainfall events. Related findings have been reported by Mearns et al. (1996, 1997), Riha et al. (1996), and Knapp et al. (2002). The latter ones, in particular, have investigated the response of a Kansas mesic grassland to changes in the rainfall regime during a series of a manipulative experiments. In agreement with their results, with the previous approach we found (Porporato et al. 2004, manuscript submitted to *Amer. Nat.*) that the net primary productivity decreased by about 20% when the frequency of rainfall was reduced while keeping mean total rainfall unchanged.

In order to fully describe the link between assimilation and plant conditions, the analysis needs to be complemented by suitable statistics accounting for the temporal dynamics of assimilation. One possibility is to proceed by analyzing the crossing properties of assimilation levels analogously to the methodology of Porporato et al. (2001), who employed a measure of plant water stress based on the mean intensity, duration, and frequency of the periods of soil water deficit, that is,

$$\overline{\theta} = \begin{cases} \left(\dfrac{\overline{\zeta}\, \overline{T}_{s^*}}{kT_{\text{seas}}} \right)^{\overline{n}_{s^*} r} & \text{if } \overline{\zeta}\, \overline{T}_{s^*} < kT_{\text{seas}} \\ 1 & \text{otherwise,} \end{cases} \tag{5}$$

where $\overline{\zeta}$ is the average of the static water stress, defined as

$$\zeta(t) = \left[\frac{s^* - s(t)}{s^* - s_w} \right]^q \qquad s_w < s < s^*, \tag{6}$$

where q is a measure of the nonlinearity of the consequences of water deficit on plants, $\overline{T}_{s^*}$ is the mean duration of an excursion below s^* (i.e., when the plant experiences water stress), $\overline{n}_{s^*}$ is the mean number of downcrossing of s^* during a growing season, and k and r are parameters defining the plant resistance to water stress ($k = r = 0.5$). The dynamic water stress was used to describe plant response to drought conditions in Laio

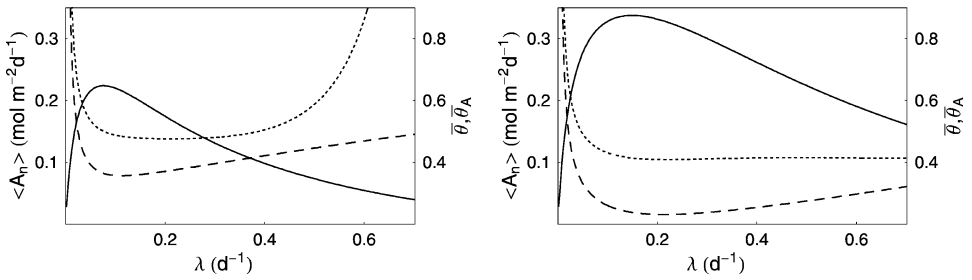

FIG. 7. Comparison of mean assimilation $\langle A_n \rangle$ (continuous line), dynamic plant water stress $\overline{\theta}$ (dotted line), and assimilation-based plant water stress $\overline{\theta}_A$ (dashed line) as a function of frequency of rainfall events for different total rainfall: (left) Θ = 50 and (right) 70 cm. Soil type is a loam with Z_r = 60 cm, T_{seas} = 200 days, k = 0.5, q = 3, and interception Δ = 0.2 cm; $E_{\max}$ = 4.3 mm day^{-1}, L_{AI} = 1.4, R_{AI} = 5.6, $A_{\max}$ = 0.68 mol m^{-2} day^{-1}, s_w = 0.29, s^* = 0.43, s_{w_A} = 0.34, and s_A^* = 0.45.

et al. (2001a), Fernandez-Illescas et al. (2001), and Porporato et al. (2003). Along the same lines, the plant water stress may also be linked to the statistics of reduction of carbon assimilation by soil moisture deficit. For this purpose, the matter is considerably simplified by the one-to-one correspondence of the crossing statistics of levels of s and A_n [see Eq. (2)]. Thus, considering that the worst plant conditions in terms of plant productivity occur when assimilation is zero, a new measure of plant stress may be defined as

$$\overline{\theta}_A = \begin{cases} \left(\dfrac{P_{A_0} \overline{T}_{s_{w_A}}}{kT_{\text{seas}}} \right)^{\overline{n}_{s_{w_A}}^{-r}} & \text{if } P_{A_0} \overline{T}_{s_{w_A}} < kT_{\text{seas}} \\ 1 & \text{otherwise,} \end{cases} \tag{7}$$

where P_{A_0} represents the average fraction of a growing season in which photosynthesis is zero, $\overline{T}_{s_{w_A}}$ is the mean duration of periods of no assimilation, and $\overline{n}_{s_{w_A}}$ is the mean number of periods of reduced assimilation.

Figure 7 shows a comparison of the mean assimilation rate and the two stress measures, with $\overline{\theta}$ directly based on water availability and $\overline{\theta}_A$ defined through the assimilation rate. Interestingly, the maximum reached by the net assimilation for both rainfall conditions does not correspond to a marked minimum in $\overline{\theta}$ and $\overline{\theta}_A$. On the contrary, and differently from $\langle A_n \rangle$, the two stresses have a wide minimum at slightly higher values of λ, suggesting that the inclusion of the threshold-crossing properties of assimilation provide a more realistic description of plant response to hydrologic fluctuations than the sole mean. This observation is also corroborated by the fact that favorable conditions for plants are not expected to be concentrated around a narrow range of parameter values, but are rather expected to change relatively slowly from optimal to nonoptimal ones (e.g., Archer 1994).

6. Conclusions

After deriving the functional dependence of the daily transpiration and carbon assimilation rates on soil moisture, the dynamics of assimilation has been coupled to the stochastic dynamics of soil moisture and studied as a function of climate, soil, and vegetation characteristics. The resulting framework has proved useful in synthesizing the impact of hydrologic processes on plant conditions. In particular, a new measure of plant stress, based on the temporal dynamics of leaf carbon assimilation, has been found to be in good agreement with the dynamic water stress defined by Porporato et al. (2001). Because of the relation between carbon assimilation and plant productivity, such a stress index may be used as a basis to assess the long-term vegetation growth as a function of climate, soil, and plant parameters as well as to help model the plant strategies to cope with water stress in conditions of interannual climatic variability.

Acknowledgments. We are grateful to John Albertson and Andrew Guswa for their useful comments. We acknowledge the support of the National Science Foundation through grants Biocomplexity (DEB-0083566) and National Center for Earth Surface Dynamics (EAR-0120914).

REFERENCES

Archer, S., 1994: Woody plant encroachment into southwestern grasslands and savannas: Rates, patterns, and proximate causes. *Ecological Implications of Livestock Herbivory in the West*, M. Vavra, W. A. Laycock, and R. D. Pieper, Eds., Society for Range Management, 13–68.

Cordoba, J. R., and R. L. Bras, 1981: Physically based probabilistic models of infiltration, soil moisture, and actual evapotranspiration. *Water Resour. Res.*, **17,** 93–106.

Crow, W. T., and E. F. Wood, 2002: Impact of soil moisture aggregation on surface energy flux prediction during SGP97. *Geophys. Res. Lett.*, **29,** 1008, doi:10.1029/2001GL013796.

Daly, E., A. Porporato, and I. Rodriguez-Iturbe, 2004: Coupled dynamics of photosynthesis, transpiration, and soil water balance. Part I: Upscaling from hourly to daily level. *J. Hydrometeor.*, **5,** 546–558.

Dingman, S. L., 1994: *Physical Hydrology*. Prentice Hall, 575 pp.

Federer, C. A., 1979: A soil–plant–atmosphere model for transpiration and availability of soil water. *Water Resour. Res.*, **15,** 555–561.

Fernadez-Illescas, C. P., A. Porporato, F. Laio, and I. Rodriguez-Iturbe, 2001: The ecohydrological role of soil texture in a water-limited ecosystem. *Water Resour. Res.*, **37,** 2863–2872.

Jarvis, P. G., 1976: The interpretation of the variations in leaf water potential and stomatal conductance found in canopies in the field. *Philos. Trans. Roy. Soc. London*, **B273,** 593–610.

Knapp, A. K., and Coauthors, 2002: Rainfall variability, carbon cycling, and plant species diversity in a mesic grassland. *Science*, **298,** 2202–2205.

Laio, F., A. Porporato, C. P. Fernandez-Illescas, and I. Rodriguez-Iturbe, 2001a: Plants in water-controlled ecosystems: Active role in hydrologic processes and response to water stress. IV. Discussion of real cases. *Adv. Water Res.*, **24,** 745–762.

——, ——, L. Ridolfi, and I. Rodriguez-Iturbe, 2001b: Plants in water-controlled ecosystems: Active role in hydrologic processes and response to water stress. II. Probabilistic soil moisture dynamics. *Adv. Water Res.*, **24,** 707–723.

Larcher, W., 1995: *Physiological Plant Ecology*. 3d ed. Springer, 509 pp.

Leuning, R., 1990: Modeling stomatal behavior and photosynthesis of *Eucalyptus grandis*. *Aust. J. Plant Physiol.*, **17,** 159–175.

——, 1995: A critical appraisal of a combined stomatal-photosynthesis model for C_3 plants. *Plant Cell Environ.*, **18,** 339–355.

Mearns, L. O., C. Rosenzwieg, and R. Goldberg, 1996: The effect of changes in daily and interannual climatic variability on CERES-WHEAT: A sensitivity study. *Climatic Change*, **32,** 257–292.

——, ——, and ——, 1997: Mean and variance change in climate scenarios: Methods, agricultural applications, and measures of uncertainty. *Climatic Change*, **35,** 367–396.

Paruelo, J. M., and O. Sala, 1995: Water losses in the Patagonian steppe: A modeling approach. *Ecology*, **76,** 510–520.

Porporato, A., and I. Rodriguez-Iturbe, 2002: Ecohydrology—A challenging multidisciplinary research perspective. *J. Hydrol. Sci.*, **47,** 811–821.

——, F. Laio, L. Ridolfi, and I. Rodriguez-Iturbe, 2001: Plants in water-controlled ecosystems: Active role in hydrologic processes and response to water stress. III. Vegetation water stress. *Adv. Water Res.*, **24,** 725–744.

——, F. Laio, L. Ridolfi, K. K. Caylor, and I. Rodriguez-Iturbe, 2003: Soil moisture and plant stress dynamics along the Kalahari pre-

cipitation gradient. *J. Geophys. Res.,* **108,** 4127, doi:10.1029/2002JD002448.
Riha, S. J., D. S. Wilks, and P. Simoens, 1996: Impact of temperature and precipitation variability on crop model predictions. *Climatic Change,* **32,** 293–311.
Rodriguez-Iturbe, I., A. Porporato, L. Ridolfi, V. Isham, and D. R. Cox, 1999: Probabilistic modeling of water balance at a point: The role of climate, soil and vegetation. *Proc. Roy. Soc. London,* **A455,** 3789–3805.
——, ——, F. Laio, and L. Ridolfi, 2001: Intensive or extensive use of soil moisture: Plant strategies to cope with stochastic water availability. *Geophys. Res. Lett.,* **28,** 4495–4497.
Scholes, R. J., and B. H. Walker, 1993: *An African Savanna.* Cambridge University Press, 306 pp.
Wetzel, P. J., and J. Chang, 1987: Concerning the relationship between evapotranspiration and soil moisture. *J. Climate Appl. Meteor.,* **26,** 18–27.
——, and ——, 1988: Evapotranspiration from nonuniform surfaces: A first approach for short-term numerical weather prediction. *Mon. Wea. Rev.,* **116,** 600–621.